System analysis of X-ray-sensitive CCDs and adaptive restoration of intraoral radiographs

Burkhard Peters[1], Dietrich Meyer-Ebrecht[1], Thomas Lehmann[2], Walter Schmitt[3]

[1]Institute for Measurement Technology
[2]Institute of Medical Informatics and Biometry
[3]Clinic of Oral and Maxillofacial Surgery

The Aachen University of Technology, D-52056 Aachen, Germany

ABSTRACT

An adaptive Wiener-filter image restoration approach is being described. It is exemplarily applied to intraoral radiographs generated by two X-ray-sensitive CCDs, one having an additional scintillator screen. The devices' MTFs were determined by means of a slightly angulated slit according to DIN 6867/2. Noise power spectra at various exposures were measured and decomposed into quantum and detector noise with respect to the signal and noise model. Both noise power levels were proportional to the incident exposure.

Wiener filters for high, low and medium exposures were designed. Weight tables for superpositions of these filters were calculated by minimizing the mean square errors between the superposition MTFs and Wiener filter MTFs for arbitrary exposures. The pixelwise weights depending on the local mean were calculated after a preceding lowpass filtering. The final restored images were composed from spatially invariant filtered images generated by 2D-IIR filtering. The results indicate that the presented adaptive restoration method is a promising approach with regard to both image quality and processing speed demands.

Keywords: adaptive image restoration, X-ray sensitive CCD, dental radiology, 2D IIR filters, Wiener filter, MTF measurement, quantum noise, detector noise, pixel superposition, signal and noise transfer.

1. INTRODUCTION

Image restoration suitable for medical routine requires processing methods with inherent adaptation to exposure dependent noise, and numerically efficient algorithms fulfilling the high speed demands of clinical practice[1]. Moreover, due to the high quality standards applying, adequate restoration approaches of direct digital X rays in the medical field depend on precise informations about the imaging properties of the systems concerned. Relevant parameters in this context are the spectral transfer functions and noise amounts.

A practicable and reliable procedure of measuring sections of the modulation transfer functions (MTFs) is to use a slightly angulated slit[3] according to DIN 6867/2[2]. Compared with methods using square wave patterns or edge phantoms, this method is relatively direct, because the MTFs only have to be corrected with respect to the slit width. Further advantages are the large number of samples being achieved with a single exposure and, because of thick lead shields, the small amounts of scattering.

Concerning the noise amounts at various exposures in the unprocessed X rays, it is important to know the total noise power spectra (NPS) as well as the portions of detector noise and quantum noise.

After measuring these parameters, a spectral model of the occuring image objects permits to optimally estimate the "true" primary image from the blurred and noisy one that was generated by the detector. Common and fast instruments to perform this estimation are spatially invariant restoration filters (Wiener-filters), that can be designed for fixed exposures on the basis of the above parameters. Medical X rays, on the other hand, are very complex 2D signals, consisting of continuously varying intensities. Optimum methods have to take this into account. The idea followed here is to superimpose the Wiener-filtered images with exposure dependent weights for each pixel.

X-ray sensitive CCDs for dental and maxillofacial imaging are interesting devices to test restoration procedures applicable in medical radiography, since the high dynamic ranges of typical intraoral images represent great challenges due to the essentially different absorption coefficients of teeth and tissue.

0-8194-2085-9/96/$6.00

An additional noteworthy fact is that the value of suitable processing parameters for CCDs, once determined, is more durable because of the CCDs' constant imaging characteristics not being changed by the alteration of digitization devices or film-, screen- or plate-materials.

In the following, after a short technical specification of the experimental the relevant signal and noise model is developed. Subsequently, the applied methods of measuring the MTFs and the NPS are listed. The signal adaptive pixel superposition restoration procedure is presented.

Finally, Wiener-filter approximations by 2D-IIR filters as well as intraoral radiographs serving as restoration examples represent first results of the work.

2. MATERIAL

The devices under examination were two CCDs for intraoral X-ray imaging (Sens-A-Ray, REGAM Medical Systems, Sweden), one of which having an additional scintillator screen. The sensor element dimensions are 45 x 45 µm, corresponding to a Nyquist rate of 22.2 / mm and a spatial frequency sampling limit at 11.1 lp / mm. The final digital images are available on an IBM-compatible PC and are 385 pixels wide (x-direction) and 576 pixels high (y-direction), with a gray level resolution of 8 bits per pixel.

The exposures were performed with a Siemens Heliodent MD X-ray tube having an intrinsic 1.5 mm aluminium filter. The focus-detector distance was 60 cm, the tube voltage 70 kVp.

The used tantalum slit phantom according to DIN 6867/2 had a width of 41 µm, a length of 9 mm and a thickness of 1.8 mm. It was a prototype that had been manufactured for the EU project 1423/1/0/073/83/12-BCR-D(30).

3. SIGNAL AND NOISE MODEL

The 2D pattern of differences of quantum fluence densities (QFDs) $\phi(x,y)$ entering the detector carries the information relevant to form the image. Thus, the spatial distribution $\Delta\phi\, o(x,y)$ of QFDs varying around a constant background level ϕ_0 is interpreted as the primary signal s to be detected and restored.

$$s(x,y) = \phi(x,y) = \phi_0 + \Delta\phi\, o(x,y) \tag{1}$$

The object-dependent 2D pattern o(x,y), i.e. the exponential projection of the object's 3D X-ray absorption properties, is characterized in the spectral domain by its 2D Fourier transform, the object spectrum O(u,v), where u and v are the spatial frequencies in x- and y-direction, respectively. Since the visibility of small details versus the local background QFD is an important criterion in medical diagnostic imaging, in the following concept the local aspect will be emphasized. Regarding a certain image region with a constant background level, corresponding to a weighted Dirac-pulse at (0,0) in the spatial frequency domain, the local total signal amplitude spectrum S of that region is the Fourier transform of (1):

$$S(u,v) = \phi_0\, \delta(0,0) + \Delta\phi\, O(u,v), \tag{2}$$

with a signal power spectrum

$$S^2(u,v) = \phi_0^2\, \delta(0,0) + [\Delta\phi\, O(u,v)]^2. \tag{3}$$

The most interesting signals are those having a relatively small contrast $\Delta\phi$ against their surrounding background and therefore being close to the detection threshold. Consequently, the model was optimized with regard to signals not having a substantial deviation from the local background QFD.

Describing the transition of the primary signal to the digital image by a one stage model as shown in Fig. 1 yields an image signal

$$s'(x,y) = \gamma\, \alpha\, [\, \phi_0 + h_d(x,y) * o(x,y)\, \Delta\phi\,], \tag{4}$$

primary image	absorption	detector transfer	detector noise	digital image
signal amplitude spectrum				
$\phi_0\delta(0,0)+\Delta\phi\ O(u,v)$			$\gamma\alpha[\phi_0\delta(0,0)+H_d(u,v)\Delta\phi\ O(u,v)]$	
signal power spectrum				
$\phi_0^2\delta(0,0)+[\Delta\phi\ O(u,v)]^2$			$\gamma^2\alpha^2\{\phi_0^2\delta(0,0)+[H_d(u,v)\Delta\phi O(u,v)]^2\}$	

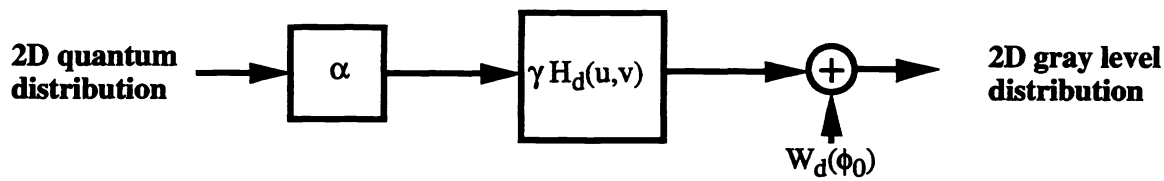

noise power spectrum

$W_q = \phi_0$ $\qquad\qquad$ $\gamma^2 H_d^2(u,v)\ \alpha\ \phi_0 + W_d(\phi_0)$

Fig. 1. signal and noise model

where γ denotes the sensitivity of conversion of QFDs into gray levels, α the detector's absorption coefficient, h_d the detector's point spread function (PSF) and * the 2D convolution operator. The corresponding signal amplitude and power spectra in the image are

$$S'(u,v) = \gamma\,\alpha\,[\,\phi_0\,\delta(0,0) + H_d(u,v)\,\Delta\phi\,O(u,v)\,], \tag{5}$$

$$S'^2(u,v) = \gamma^2\,\alpha^2\,[\,\phi_0^2\,\delta(0,0) + \{\,H_d(u,v)\,\Delta\phi\,O(u,v)\,\}^2\,], \tag{6}$$

with H_d denoting the detector MTF.

The quantum noise W_q in the primary image can be modeled as a white process with a power being equal to the local mean QFD ϕ_0, and $\alpha\phi_0$ before and after the absorption stage, respectively. The quantum NPS is modified by the detector MTF. Additional noise is introduced by CCD read-out and A/D-conversion, i.e. electronic and quantization noise having a white spectrum. The total noise W_{tot} in the final image can therefore be split up into a quantum noise part W_q' being proportional to the square of the MTF, and a white detector noise part W_d.

$$W_{tot} = W_q'(u,v) + W_d = \gamma^2\,\alpha\,H_d^2(u,v)\,\phi_0 + W_d \tag{7}$$

The model permits the detector noise part to have an arbitrary dependency on the incident exposure.

4. MTF MEASUREMENTS

Before measuring the spectral transfer functions, both devices' total sensitivity functions were measured by taking X rays at continuously ascending exposures from 0.01 through 0.2 mAs and determining the mean gray levels. It has to be mentioned that, in this context, it will be sufficient to know the characteristic curves in units of gray levels per mAs. The linearity of the tube's X-ray emission had been verified previously. The measurements showed a nearly perfect proportionality between exposure and mean gray level for both devices (Fig. 2). The scintillator device turned out to have a slightly higher γ than the CCD.

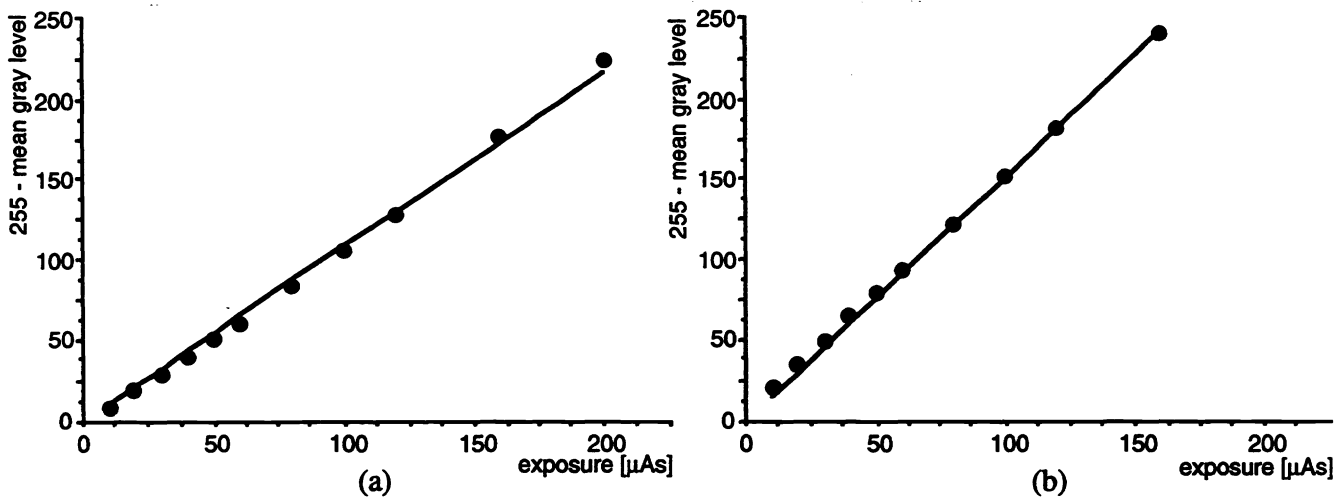

Fig. 2. Measured characteristic curves and linear approximations, 70 kVp, 1.5 mm Al, 60 cm focus-detector, (a) CCD sensor, (b) Scintillator device

Finely sampled line spread functions (LSFs) were determined from several slit images, with slits having a slight angle to the selected direction, at varying positions on the device. Within the range of measurement precision, the measured LSFs were identical, thus justifying the assumption of spatial invariance. The applied method of determining the MTF had been proposed elsewhere for the analysis of the spectral transfer properties of a storage phosphor system[3]. In the case of the investigated CCDs it yielded well reproducible MTFs. A practical restriction to be mentioned was the necessity to leave at least one exposure indicator in the device uncovered with lead when using automatic acquisition mode. Measurements with full lead shields outside the slit area therefore had to be performed in manual acquisition mode. However, scattering did not appear to corrupt the auto mode measurements, so the partial shielding seemed to be sufficient for this purpose. Taking into account the slit transfer as a convolution with

$$\text{rect}(x/w) = \begin{cases} 1 & \text{if } |x| < 0.5\,w \\ 0 & \text{else,} \end{cases} \tag{8}$$

the measured MTF sections had to be corrected by division through $\text{sinc}(\pi w f) = \sin(\pi w f) / (\pi w f)$, where x denotes the actual space coordinate, f the corresponding spatial frequency and w the slit width. The complete 2D MTFs were approximated from the 1D sections by cubic interpolation along circles, with first derivatives set to zero on the vertical and horizontal axes. From lower to higher frequencies, the CCD MTF was found to be a continuously decreasing function with an essentially anisotropic characteristic, i.e. worse transfer capabilities in x- than in y-direction (Fig. 3a). The scintillator MTF is continuously decreasing as well, but isotropic and, in comparison with the CCD MTF, with reduced transfer factors in the low frequency range (Fig. 3b). Towards higher frequencies the MTF is nearly congruent with the CCD MTF in x-direction. The results of the MTF measurement were similar to those obtained by square wave response methods[4].

5. NOISE ANALYSIS

The scope of the noise analysis was to achieve a global model of the involved noise amounts as a basis for an adaptive image restoration approach. Therefore it was intended to determine the frequency and signal amplitude dependencies as a whole rather than a certain single noise amount. For this reason, noise measurements covering the whole dynamic range were performed for both devices with stepwise increasing

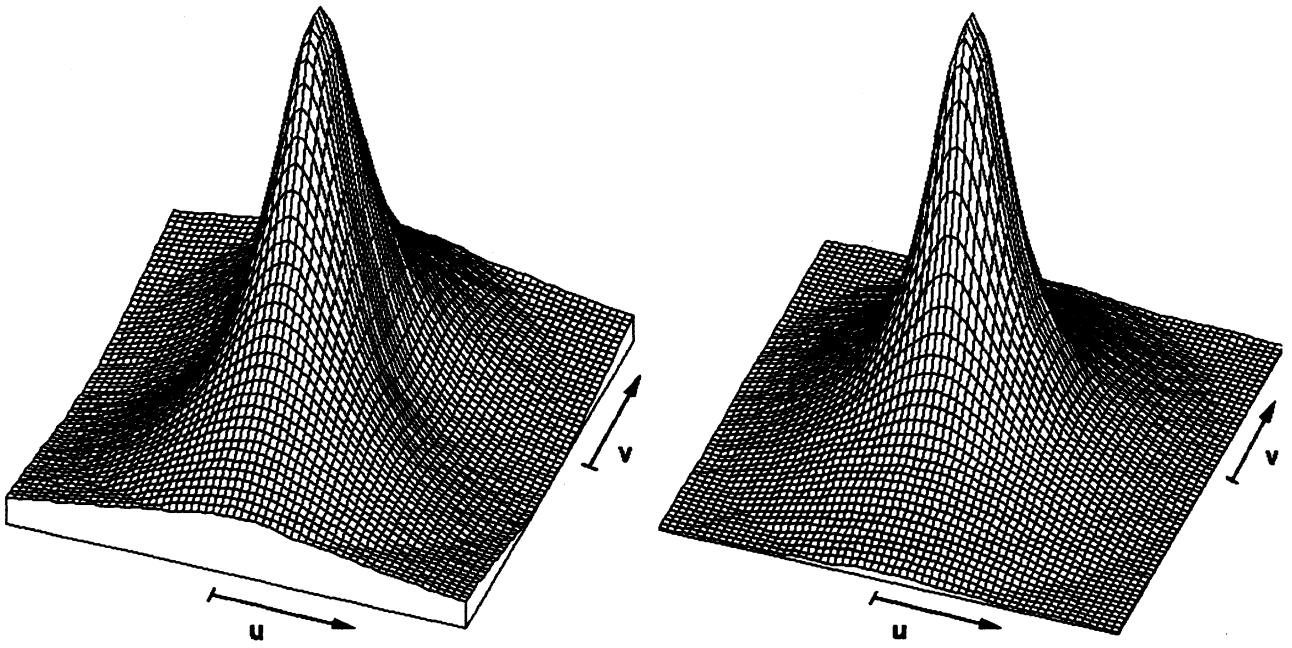

(a) (b)

Fig. 3 MTFs interpolated from sections determined by means of an angulated slit, u and v spatial frequencies corresponding to x- and y-direction, respectively, (a) CCD sensor, (b) Scintillator device

exposures from 0.01 through 0.2 mAs. From each of the uniformly exposed plain images 45 subframes à 64 x 64 pixels were extracted. The margins of the images were excluded when cutting the subframes because of their sometimes significantly different mean gray levels. The length of 64 pixels was sufficient to determine 33 independent samples of the NPS in the respective direction. The width of 64 pixels was the dimension necessary to get a section rather than a projection of the NPS, which can be easily derived from the scanning slit dimensions needed in analysis of analogue imaging systems[5]. In contrast to those analyses the noise calculation was not done after averaging in the spatial domain but, principally equivalent, in the spectral domain, using the inherent projection property of the 2D Fourier transformation.

All of the subframes were 2D Fourier-transformed, squared, and normalized according to the subframe dimension. Final ensemble averaging over all subframes belonging to a certain exposure yielded the estimate of the adjacent 2D NPS. The NPS sections in horizontal and vertical directions were extracted. According to the noise model, these sections had to represent linear combinations of the respective MTF sections' squares and white detector noise portions. Since only one image per exposure had been acquired, the statistical measurement error naturally was quite high for the single exposure. Therefore a robust linear fitting procedure was suitable to determine the levels of quantum and detector noise. As can be seen from the fitting results in Figs. 4 and 5, the model holds for both devices, both directions and irrespectively of the exposure.

In Figs. 6 and 7, for both devices the quantum and detector noise power levels resulting from this fitting procedure were plotted versus the incident exposure. As expected from the signal and noise model, the quantum noise power level increased proportional to the exposure. In addition, the detector noise power level was proportional to the exposure, too. For both devices, the total noise therefore can be described by

$$W_{tot} = W_q' + W_d = \phi_0 (W_{q0}' + W_{d0}), \tag{9}$$

where $W_{q0}' = \alpha \gamma^2 H_d^2(u,v)$ and $W_{d0} = W_d / \phi_0 = \text{const.}$

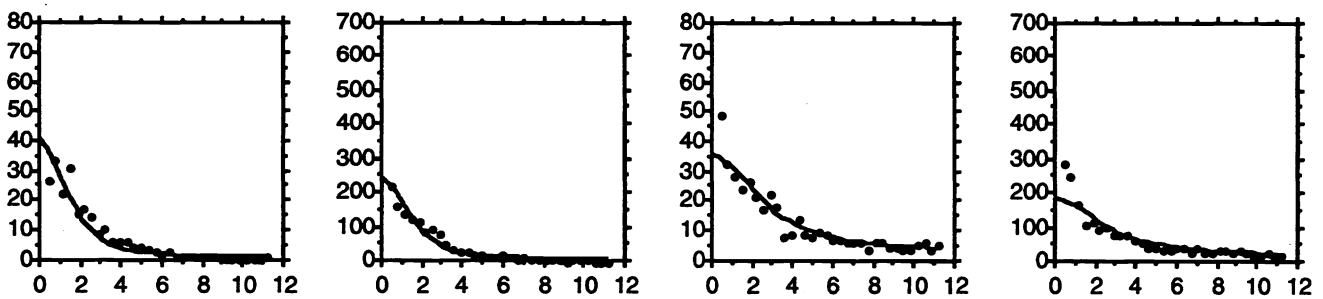

Fig. 4. CCD sensor: Measured NPS (full points) and model-based fitted curves, 70 kVp, 1.5 mm Al, distance focus-detector 60 cm, noise in units of gray levels vs spatial frequency in lp/mm, (a) horizontal 0.03 mAs, (b) horizontal 0.12 mAs, (c) vertical 0.03 mAs, (d) vertical 0.12 mAs

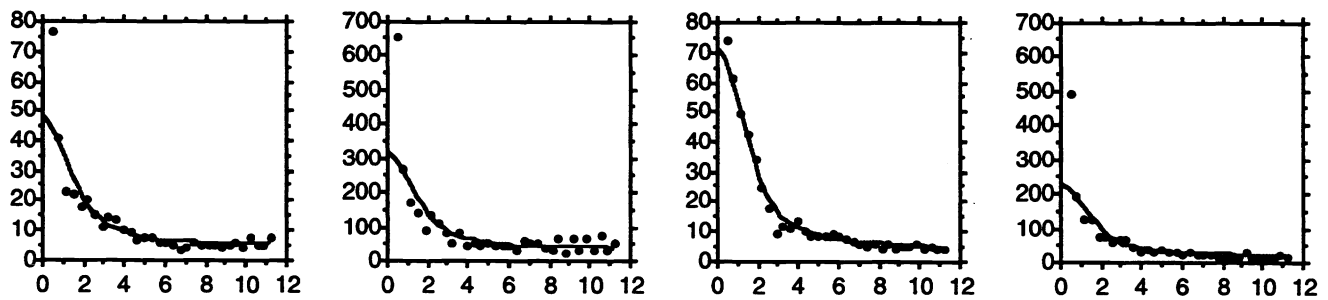

Fig. 5. Scintillator device: Measured NPS (full points) and model-based fitted curves, 70 kVp, 1.5 mm Al, distance focus-detector 60 cm, noise in units of gray levels vs spatial frequency in lp/mm, (a) horizontal 0.03 mAs, (b) horizontal 0.12 mAs, (c) vertical 0.03 mAs, (d) vertical 0.12 mAs

6. ADAPTIVE RESTORATION

The common invariant 2D Wiener filter approach[6] estimates the original image signal s on the basis of the available blurred and noisy image s' optimally in the least squares sense: $E\{ (s - s'')^2 \} \rightarrow \min$, where $s'' = s' * h_w$ is the restored image and h_w the Wiener filter PSF. To design the Wiener filter, one has to know the system's PSF or OTF, and the total NPS contained in the image to be restored. Additionally, one has to estimate the actual object spectrum O of the items represented in the image, and the absolute ratio of signal and noise powers. The required Wiener filter is specified in the frequency domain by its MTF

$$H_w(u,v) = \frac{1}{H_d(u,v)} \frac{S^2(u,v)\,|H_d(u,v)|^2}{S^2(u,v)\,|H_d(u,v)|^2 + W_{tot}(u,v)} \qquad (10)$$

Using (2), (7) and (9) yields

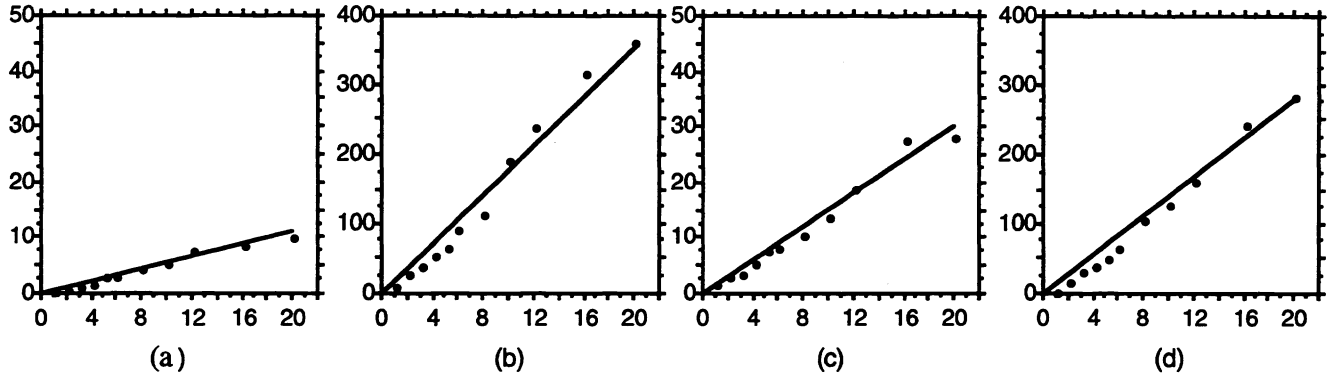

Fig. 6. CCD sensor: noise power levels vs exposure [in 10 μAs] derived from measurements by model-based fitting, conditions as in Figs. 2 and 3, (a) detector noise power level, horizontal, (b) quantum noise power level, horizontal, (c) detector noise power level, vertical, (d) quantum noise power level, vertical

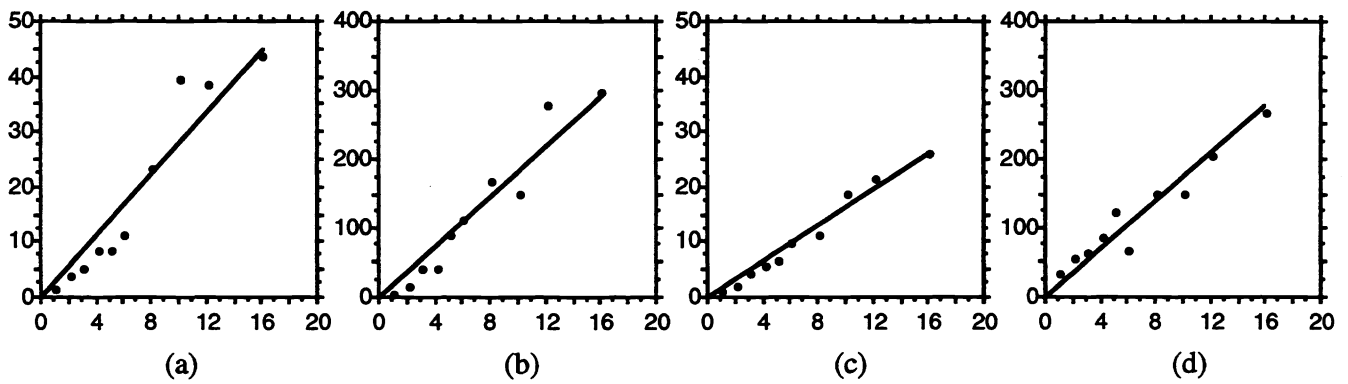

Fig. 7. Scintillator device: noise power levels vs exposure [in 10 μAs] derived from measurements by model-based fitting, conditions as in Figs. 2 and 3, (a) detector noise power level, horizontal, (b) quantum noise power level, horizontal, (c) detector noise power level, vertical, (d) quantum noise power level, vertical

$$H_w(u,v) = \frac{1}{H_d(u,v)} \frac{[\Delta\phi\, O(u,v)]^2\, |H_d(u,v)|^2}{[\Delta\phi\, O(u,v)]^2\, |H_d(u,v)|^2 + \phi_0\, [\alpha\, \gamma^2\, H_d^2(u,v) + W_{d0}]} \quad ,u+v \neq 0 \qquad (11)$$

The noise part is depending linearly on the exposure ϕ_0 while the signal part increases quadratically with $\Delta\phi$, which itself is proportional to ϕ_0. Recognizing the fact that a radiographic image, in general, consists of locally different exposures, it is obvious that an invariant Wiener filter always is optimal only for a constant local ratio $\Delta\phi$ / ϕ_0, i.e. for a selected exposure ϕ_0. Superimposing an invariantly filtered image with the unprocessed image according to the pixel intensity[7] is simple but might be to coarse. Designing a filter bank with specialized filters for some exposures and switching the coefficients pixel by pixel[8] according to the nearest neighbor filter runs the risk of introducing artifacts at the switching points.

To avoid abrupt switches, it is proposed here to realize smooth spatial transitions of the applied filter characteristic. To insure this, a smoothed version of the raw image s' is generated by lowpass filtering, serving as transition matrix. To achieve a good compromise between local adaptivity and smoothness, the dimension of the used Gaussian lowpass filter kernel has to be adapted to the spatial expansion of the

designed Wiener-filters' PSFs. Subsequent inversion of the smoothed image yields an image representing a good estimate for each pixel's surrounding mean QFD.

A specialized Wiener-filter for each actual QFD is now approximated by superposition of the two available Wiener filters designed for the nearest upper and lower QFDs.

$$H_w \approx a\, H_{wu} + b\, H_{wl} \tag{12}$$

The superposition weights a and b are determined previous to the restoration procedure by MSE minimization according to

$$E\{\, \Theta(f)\, [H_w - (a\, H_{wu} + b\, H_{wl})]^2 \,\} \rightarrow \min. \tag{13}$$

The weight function $\Theta(f)$ is selected to be reciprocally proportional to the spatial frequency because, in general, it is more important to achieve a good approximation of the lower frequency part. The weights as well as the nearest neighbor filters to be selected are equal for all pixels of the same level. Storing these informations in level-oriented LUTs (lookup-tables) saves computational expense.

Once having calculated the mean QFD image and knowing the LUT containing the weights and neighbors depending on the QFDs the adaptive Wiener filter restoration can be performed in a straigthforward and computationally efficient way.

The available spatially invariant Wiener-filters are applied separately to the raw image s', each of them yielding optimum restorations only in those image regions exactly matching the mean QFD the filter had been designed for. At this moment, it is a precondition for deriving a single, correctly restored image with a continuous adaptivity to the local QFD to have applied only linear operators with zero phase MTFs. The described Wiener-filter approximation by weighted superposition of available filters is now performed in the spatial domain and following the invariant filter operation. The resulting synthesized filter characteristic, in general, is pixelwise smoothly changing and always representing the optimum combination of the invariant filtered local signals. The procedure is described in the spatial domain by

$$s'' = s' * h_w \approx a\,(s' * h_{wu}) + b\,(s' * h_{wl}) = s' * (a\, h_{wu} + b\, h_{wl}) \tag{14}$$

and in the spectral domain by

$$S'\, H_w \approx a\, S'\, H_{wu} + b\, S'\, H_{wl} = S'\,(a\, H_{wu} + b\, H_{wl}). \tag{15}$$

This signal-adaptive way to compose a restored image, of course, may be adapted to individual preferences regarding processing speed and accuracy. The number of images to be superimposed, minimum two, is to be selected as well as the concrete implementation of the spatially invariant Wiener-filters, e.g. IIR- or FIR-convolution in the spatial domain or filtering in the spectral domain. Practical tests showed that an amplitude scaling of the final image is well performed generating an affinity between the histograms of the initial and the resulting image.

7. RESULTS

The used spatially invariant Wiener-filters were designed by means of genetic algorithms[9] as 2nd through 4th order 2D-IIR filters, depending on the approximation quality. Zero phase filter MTFs were realized by a cascade algorithm, consecutively traversing the image in the four diagonal directions. For low exposures yielding smoother Wiener-filter MTFs 2nd order filters were sufficient in any case. The filters for high exposures had to have pronounced shapes even at lower spatial frequencies corresponding to more expanded PSFs and therefore often were better approximated by higher order filters. Sample approximations are presented in Figs. 8a through 8d.

Even though recursive filtering is more efficient than FIR-filtering the main computational expense of the procedure is still due to the spatially invariant Wiener-filtering. If N invariantly Wiener-filtered images of

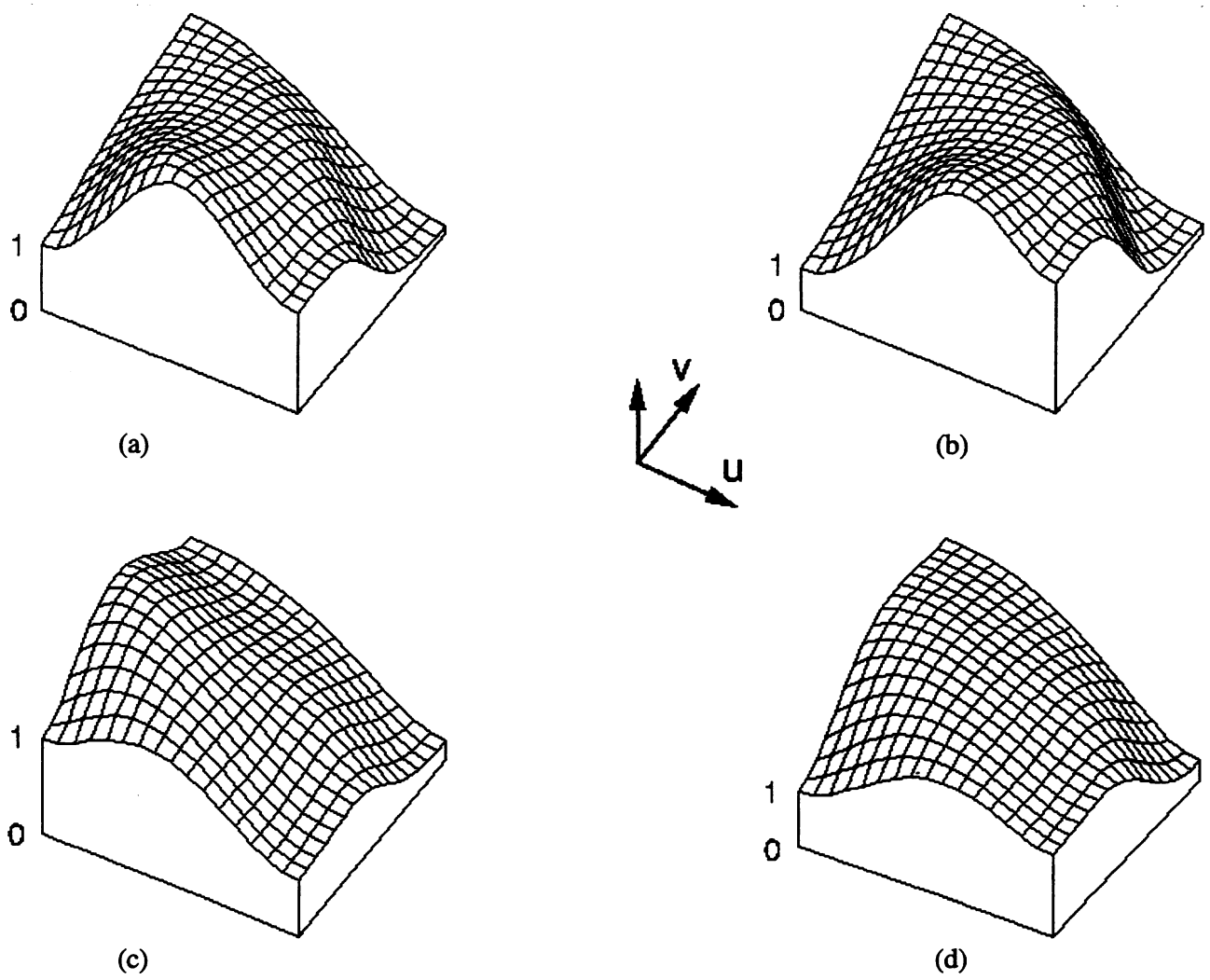

Fig. 8. Quarterplanes of MTFs of sample Wiener-filter approximations by 2D-IIR filters having zero phase due to the cascade algorithm, (a) CCD sensor, mean gray level = 240, (b) CCD sensor, mean gray level = 38, (c) Scintillator device, mean gray level = 240, (d) Scintillator device, mean gray level = 12

dimensions X and Y (X=375, Y=576 in case of the Sens-A-Ray devices) and one mean-QFD image are to be generated by means of the cascaded 2D-IIR-filter algorithm with filters orders O_f, then

$$N_{mult1} = 4\,(N+1)\,X\,Y\,[2(O_f+1)^2-1] \tag{16}$$

multiplications and the same number of additions must be performed. Additionally, $N_{mult2} = 2\,X\,Y$ multiplications and half as many additions are necessary to produce the final image, yielding a total computing time for the arithmetic operations of

$$T_a = \{\,4\,(N+1)\,[2(O_f+1)^2-1] + 2\,\}\,X\,Y\,T_{mult} + \{\,4\,(N+1)\,[2(O_f+1)^2-1] + 1\,\}\,X\,Y\,T_{add}. \tag{17}$$

Using only three invariant filtered images and performing all filter operations by 2nd order filters, the restoration of an X ray generated by a Sens-A-ray device takes about 60×10^6 multiplications and nearly the

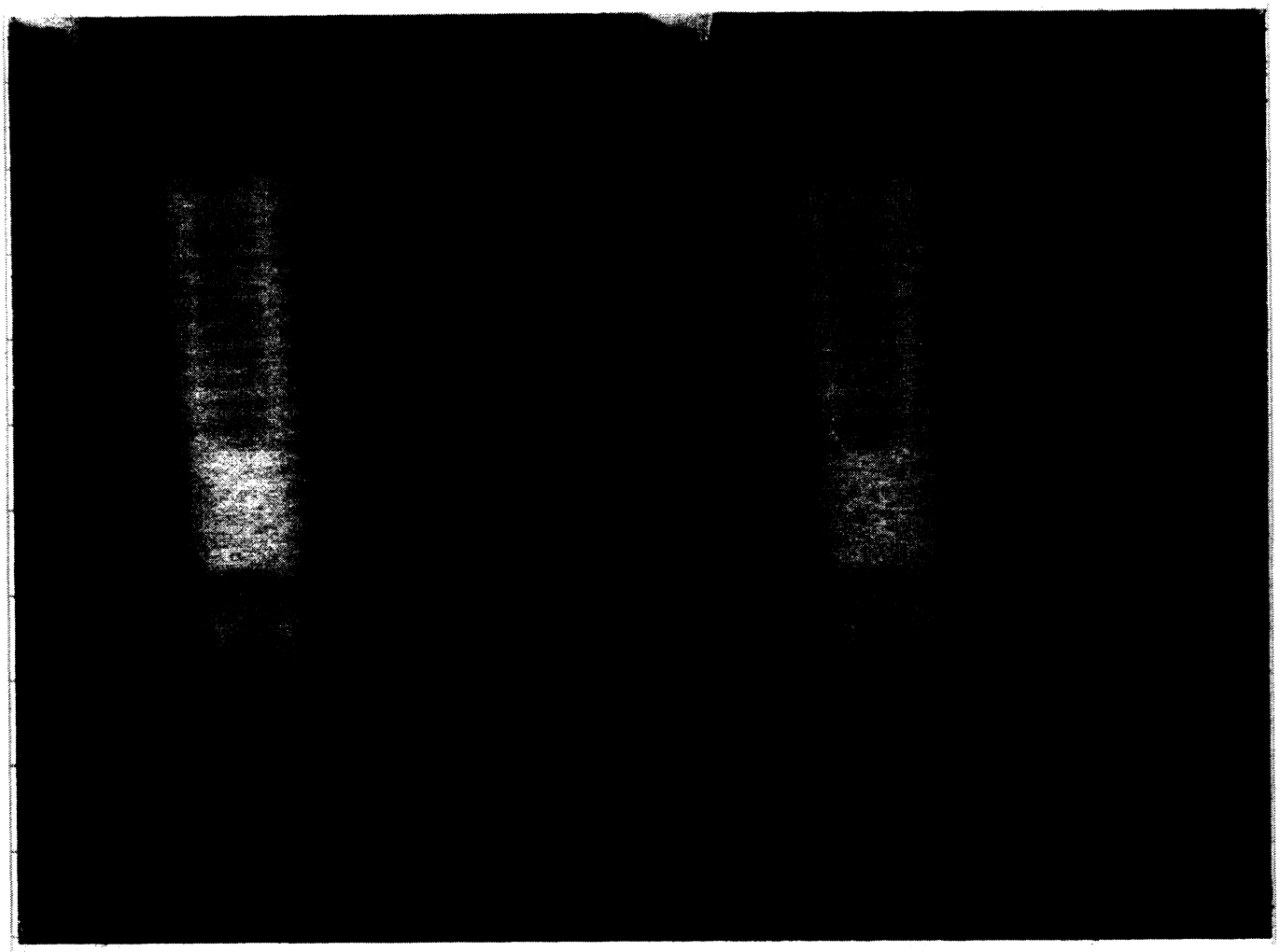

(a) (b)

Fig. 9. Dental radiograph with implant, generated by the CCD sensor, (a) raw image, (b) restored image

same amount of additions.

The restored images show clearly the MTF-compensating effect of the technique. When comparing them with the invariantly filtered images, the superimposed resulting images combine their advantages in the low, medium and high exposure regions, respectively. The method's performance will be initially tested as a preceding stage to edge extraction and identification of dental implants[10] as shown in the sample radiographs Figs. 9a and 10a. In Figs. 9b and 10b, it can clearly be seen that the implant edges have become sharper while no edge-artifacts were introduced, indicating the method's suitability for this application. Homogeneously low exposed regions as, for example, the implant areas, appear somewhat noisier in the restored images. This fact indicates that the additional adaptation of the filter characteristic to the local homogeneity of the image might be a step towards further improvement of the method.

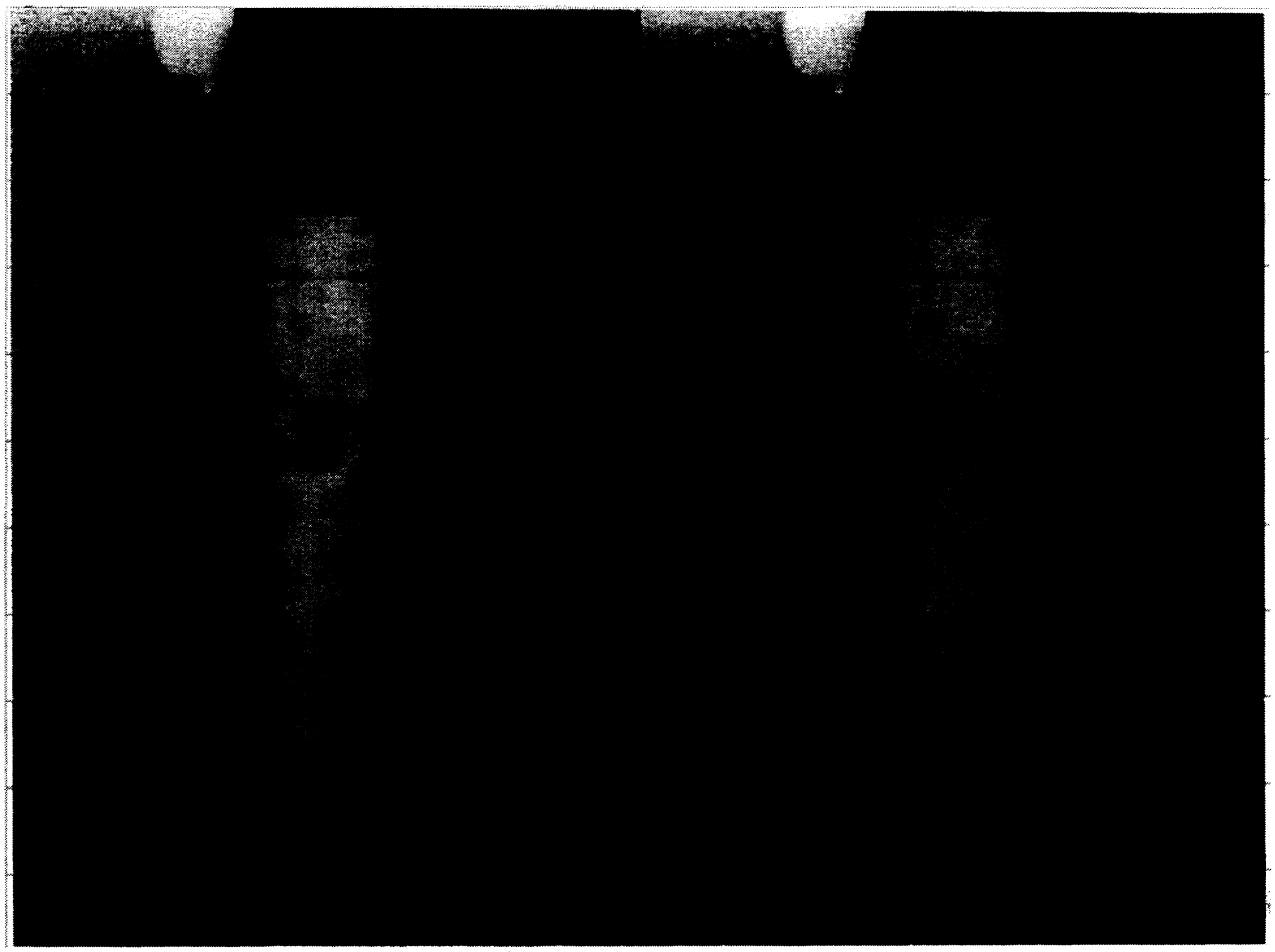

(a) (b)

Fig. 10. Dental radiograph with implant, generated by the scintillator device, (a) raw image, (b) restored image

8. CONCLUSION

A continuously adaptive Wiener-filter technique for image restoration working by pixelwise superposition of invariant filtered images has been presented. The algorithm is of a non-iterative type and may be adapted to individual preferences by either selecting higher processing speed or higher restoration accuracy. The promising first results gained by application in CCD-based medical X-ray-imaging give motivation to enhance the method's performance by introduction of typical object spectra and to go ahead with its clinical evaluation.

9. ACKNOWLEDGEMENTS

The authors wish to thank Prof. D. Hoeschen of the PTB (Physikalisch-Technische Bundesanstalt) Braunschweig, Germany and Mr. P. Quadflieg of Philips Research Laboratories Aachen, Germany for their advice and material support concerning the MTF measurements.

10. REFERENCES

1. Meyer-Ebrecht D., "Digital image communication", European Journal of Radiology, Vol. 17, pp. 47-55, 1993.

2. DIN 6867 Teil 2: *Bildregistrierendes System, bestehend aus Röntgenfilm, Verstärkungsfolien und Kassette zur Verwendung in der medizinischen Röntgendiagnostik (Bestimmung der Modulationsübertragungsfunktion)*, Beuth-Verlag, Berlin, 1991.

3. H. Fujita, D.Y. Tsai, T. Itoh, K. Doi, J. Morishita, K. Ueda, A. Ohtsuka, "A simple method for determining the modulation transfer function in digital radiography", IEEE Trans. on MI, Vol. MI-11, No. 1, pp. 34-39, March 1992.

4. W. Hillen, J. Bockemühl and W. Schmitt, "Signal-to-noise performance of a digital X-ray detector", *Proceedings of the International Symposium CAR' 95, Computer Assisted Radiology*, eds. H.U. Lemke, K. Inamura, C.C. Jaffe, and M.W. Vannier, pp. 990-995, Springer-Verlag, Berlin, 1995.

5. J.C. Dainty and R. Shaw, *Image Science*, pp. 292-298, Academic Press, London, 1974.

6. W.K. Pratt, *Digital Image Processing*, pp. 410-415, John Wiley & Sons, New York, 1978.

7. S. Rupp, *Digitale Radiographie - Optimierung der Bildqualität durch Bildverarbeitung*, Fortschrittberichte VDI, Reihe 10: Informatik/Kommunikationstechnik, Nr. 161, pp. 107-109, VDI-Verlag, Düsseldorf, 1991.

8. F.M. Wahl, *Digitale Bildsignalverarbeitung*, pp. 117-120, Springer-Verlag, Berlin, 1984.

9. T. Lehmann, W. Schmitt, M. Horn, W. Hillen, "IDEFIX - Identification of dental fixtures in intraoral X rays", *Medical Imaging* , M.H. Loew, K.M. Hanson, Proc. SPIE 2710 (this issue), paper 2710-58, 1996.

10. B. Peters and B. Wein, "An Interactive System for High-Speed X-Ray Image Filtering", *Proceedings of the International Symposium CAR' 93, Computer Assisted Radiology*, eds. H.U. Lemke, K. Inamura, C.C. Jaffe, and R. Felix, pp. 298-302, Springer-Verlag, Berlin, 1993.